

Structural and magnetic properties of nickel substituted cobalt ferrite nanoparticles by Sol-gel method

Sandhya Bharambe¹, Pushpinder Bhatia², Umesh Shinde³

¹Department of Physics, Guru Nanak College of Arts, Sciences and Commerce, 400037 Mumbai, Maharashtra, India

²Department of Physics, Guru Nanak College of Arts, Sciences and Commerce, 400037 Mumbai, Maharashtra, India

³Department of Humanities and Applied Sciences, K. J. Somaiya Institute of Engineering and Information Technology, Maharashtra, India

ABSTRACT

The structural parameters of nickel-substituted cobalt ferrite nano-particles $Ni_xCo_{1-x}Fe_2O_4$ ($x=0, 0.2, \text{ and } 1.0$) synthesized using sol-gel method are studied. X-ray diffraction technique confirms the formation of nano-sized particles of cubic spinel structure. Lattice parameters, density, crystallite size and hopping lengths are determined while FT-IR transmission spectra and scanning electron microscope images are studied. The magnetic properties were confirmed by the use of electron spin resonance spectroscopy and peak-to-peak line width, resonant magnetic field and the g-factor are also measured. The observed g-value from ESR agrees with the standard value. FT-IR transmission spectra for samples confirm the spinel structure arising from tetrahedral and octahedral interstitial sites in the crystal of ferrites. A cationic exchange between the lattices is revealed.

Keyword: - Nickel Cobalt ferrite nanoparticles, spinel, IR spectroscopy, Scanning Electron Microscope, Electron spin resonance.

1. INTRODUCTION

Magnetic nano-particles of spinel ferrites are of great interest for addressing the fundamental relationship between magnetic properties and their crystal chemistry and structure. Among various types of NPs, spinel ferrites with a general formula of (MFe_2O_4) , $M = Co^{2+}, Ni^{2+}, Fe^{2+}, Zn^{2+}, Cu^{2+}$ etc) nanocrystals raised as a novel group of nanomaterials in chemical, electrical, structural, mechanical Magnetic properties[1-2] Their physical properties such as high magnetic permeability and high electrical resistance make them useful for applications in magnetic storage devices, microwave and electronic devices, etc.[3]. Applications of ferrites are seen in diverse fields such as drug delivery in biomedical field [4-5], catalysts [6], magneto-optical devices [7], semiconducting gas sensor[8]. Nanoparticles as adsorbents for heavy metal ions are an emerging area of research, too [9]. Their insolubility in water and high surface area can make them potential adsorbents for the removal of contaminants from polluted water [10] They also have superparamagnetic properties and high surface to volume ratio[10].

In recent years, a number of chemical and physical methods have been attempted to produce nanosize ferrites. Some of the different ways of preparing the nanoparticles are co-precipitation method [11] combustion process[12] hydrothermal synthesis [13] microemulsion method [14], ball milling[15],and sol-gel method[16]. Most of these methods have achieved particles of the required size and shape, but they are impractical for large-scale applications because of they require expensive and complicated procedures, high reaction temperatures, long reaction times, and toxic reagents. They also produce toxic by-products that may harm the environment [17]

In the present study Nickel-substituted Cobalt ferrites are prepared through sol-gel method and a comparison is made by studying the structural properties of nanoparticles. The obtained nanoparticles are characterized using X-ray diffraction(XRD), Scanning electron microscopy (SEM), FT-IR transmission spectra and Electron spin resonance (ESR) at room temperature.

2. EXPERIMENTAL

2.1 Synthesis

Nickel-substituted cobalt Ferrite $\text{Ni}_x\text{Co}_{1-x}\text{Fe}_2\text{O}_4$ ($x=0, 0.2, \text{ and } 1.0$) have been synthesized by sol-gel method. All the reagents used for the synthesis of Nickel-substituted cobalt ferrite nano-particles were of analytical grade (99.9% purity). Stoichiometric amounts of ferric nitrate $\text{Fe}(\text{NO}_3)_3 \cdot 9\text{H}_2\text{O}$, cobalt nitrate $\text{Co}(\text{NO}_3)_2 \cdot 6\text{H}_2\text{O}$ and nickel nitrate $\text{Ni}(\text{NO}_3)_2 \cdot 6\text{H}_2\text{O}$ dissolved in distilled water. Around 5 ml of nitric acid is added to form the homogeneous solution and to maintain the pH between 2 and 3. Solution is heated on hot plate for half an hour then citric acid is added to solution. After getting sol on slow evaporation, a gelating reagent ethylene glycol was added and heated around 100°C to get a gel. The gel on further heating in oven at 200°C around 12 hours yields a dry fluffy porous mass, which was calcined at 700°C for 3 hours. These Nickel-substituted Cobalt ferrite powder samples are designated as S1(CoFe_2O_4), S2($\text{Ni}_{x0.2}\text{Co}_{0.8}\text{Fe}_2\text{O}_4$), S3 (NiFe_2O_4) ($x=0, 0.2, 1.0$) respectively.

2.2 Measurements

The structural characterization is performed by X-ray diffractometer (XRD) using Bruker D8 advance (operated at 40 kV and 40 mA). The measurements are taken at RT with Cu as anode material and the $\text{K}\alpha$ radiation of wavelength 1.5406\AA as the incident/diffracting wave. Scanning Electron Microscope (SEM, JEOL –JSM-6380, LA with EDX) was used in order to investigate the nanostructure, morphology and elemental composition of the sample. All samples were recorded in $4000\text{--}400\text{ cm}^{-1}$ region at ambient temperature using FT-IR transmission spectra (Bruker, Germany, 3000 Hyperion Microscope) Spectrometer. Magnetic resonance (ESR) spectrometer (JEOL, Japan, JES-FA200 Spectrometer) at a frequency of about 9.65 GHz were carried out on finely powder samples at room temperature.

3. RESULTS AND DISCUSSION

3.1 Structural characterization

Fig.1 shows the X-ray diffractometer (XRD) patterns of Nickel-substituted cobalt Ferrite of S1, S2, S3 ($x=0, 0.2, \text{ and } 1.0$) samples. Spinel structure of annealed powders of the Nickel-substituted cobalt ferrite samples confirmed by the XRD patterns from JCPDS No. 22-1086 for CoFe_2O_4 and JCPDS No.74-2081 for NiFe_2O_4 for CoFe_2O_4 have been presented in Fig.1 Eight obvious diffraction peaks corresponding to (220), (311), (222), (400), (422), (511), (440) and (533) planes shows the peak positions.

The average crystallite size is calculated from the most intense peak (311) using the Scherrer's formula [18]

$$D = \frac{k\lambda}{\beta \cos\theta} \quad (1)$$

where, D is the average crystalline size, k the Scherrer constant, λ the X-ray wavelength used, β the angular linewidth of half maximum intensity and θ is the Bragg's angle in degrees unit. The results are shown in Table 1. The lattice parameter "a" of individual compositions was calculated by using the formula:

$$a = d\sqrt{h^2 + k^2 + l^2} \quad (2)$$

where (h, k, l) are the Miller indices. It has been found that the lattice parameter value decreases from 8.5495\AA for cobalt ferrite to 8.4869\AA for nickel ferrite with increasing substitution of Ni for Co. The decrease in lattice parameter with the increase in Ni^{2+} ion concentration is due to replacement of large ionic radii Co^{2+} ions (0.78\AA) by smaller ionic radii Ni^{2+} ions (0.63\AA) in the host lattice of cobalt ferrite [19]

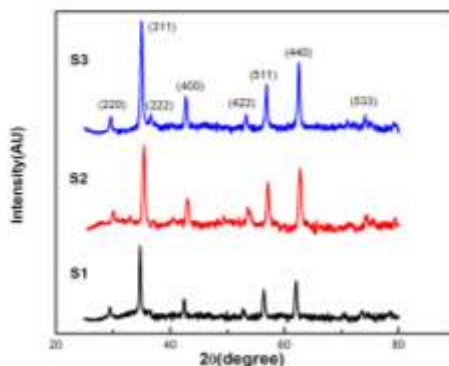


Fig -1: X-ray diffraction patterns of S1, S2, S3 ($x=0, 0.2, \text{ and } 1.0$) samples

The X-ray density (the theoretical density) ρ was calculated using the relation

$$\rho = \frac{zM}{N_A a^3} \quad (3)$$

where M is the molar mass of the ferrite, 'a' is the lattice parameter, and N_A is Avogadro's number [20] From XRD patterns and Scherrer's formula, mean crystallite sizes of the samples are found to be around 25-35 nm by sol-gel method. It is found that X-ray density increases from 4986 Kg/m³ for cobalt ferrite to 5093 Kg/m³ for nickel ferrite with increase in Nickel concentration ferrite as expected due to the smaller radius of nickel atom in comparison to the cobalt atom. Variation in lattice parameter, interplanar spacing(d) crystallite size (D), and density(ρ) with respect to increase in Ni concentration are calculated and tabulated in [Table 1] The distances between the centers of adjacent ions (hoping length) in the tetrahedral A-sites (L_A) and octahedral B-sites (L_B) is given by the following relations [21]

$$L_A = \left(\frac{\sqrt{3}}{4}\right)a \quad (4)$$

$$L_B = \left(\frac{\sqrt{2}}{4}\right)a \quad (5)$$

where a is the lattice constant.

Table 1. XRD analysis of S1,S2, S3 ($x=0, 0.2, 1.0$)

Samples	Interplanar spacing (d) Å	Lattice parameter(a) Å	Crystallite size (D)Å	Density (ρ) Kg/m ³	L_A (Å)	L_B (Å)
S1	2.5778	8.5495	2.5355	4986	3.7020	3.0227
S2	2.5623	8.4981	2.8166	5076	3.6798	3.0045
S3	2.5558	8.4869	3.3617	5093	3.6749	3.0005

3.2 SEM ANALYSIS

Fig. 2 shows SEM images of the Nickel-substituted cobalt Ferrite S1, S2, S3 ($x=0, 0.2, \text{ and } 1.0$) samples. The morphology and the size distribution of the nanoparticles are determined using SEM. In the SEM images it is observed that irregular shapes and different sizes, and the agglomeration of the grains. SEM micrograph depicts that the samples contain micrometrical aggregation of tiny particles. It can be seen that with the substitution of transition metals in ferrite phase, the agglomeration increases the existence of high dense agglomeration indicates that pore free crystallites are present on the surface.[22].

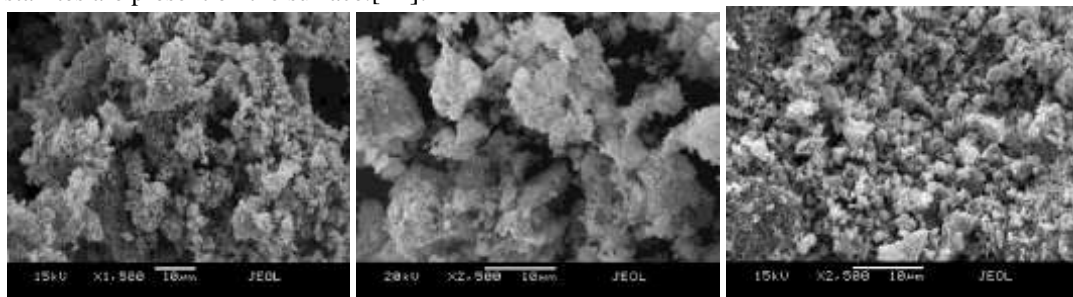


Fig.2 SEM micrographs of S1,S2,S3 samples (a) $x=0$, (b) $x=0.2$, (c) $x=1$

3.3 ESR-ELECTRON SPIN RESONANCE

The ESR of ferrites is important for investigating the magnetic properties of magnetic materials at high frequency because the resonance originates from the interaction between spin and electromagnetic waves[23]. Electron spin resonance is a technique of observing resonance absorption of microwave power by unpaired electron spins aligned with magnetic field. When the electrons are subjected to an external field H (it is customary to place the field along the z axis), the energy levels of the generate spin states split depending on their quantum magnetic moment $m_s = \pm 1/2$ and the strength of the magnetic field. The g -value is one of the most important concepts in ESR

studies[24]. All spectra exhibited broad signals, peak-to-peak line width (ΔH_{pp}), resonant magnetic field (H_r), and g-factor are three parameters that characterize the magnetic properties. Usually peaks in ESR (which have an alternating current shape) are described using g-values, which are a measure of the magnetic fields at which they occur. The room temperature electron spin resonance spectrum of samples nanocrystalline ferrites are shown in Fig3.

The values of various parameters such as peak to peak line width (ΔH_{pp}), resonance field (H_r) g-value, relaxation time(τ_2), are calculated and tabulated in Table 2

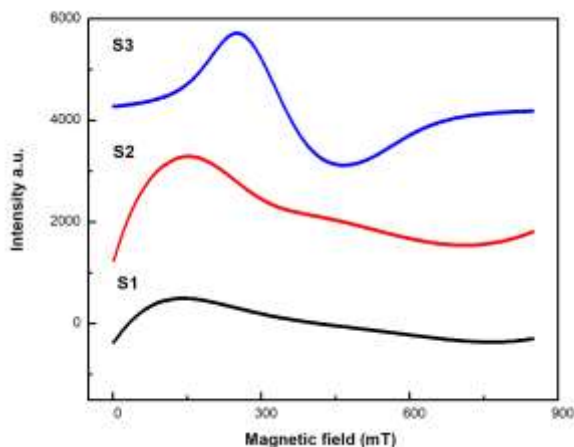


Fig. 3 ESR spectra of S1,S2,S3 (x=0, 0.2,1.0) samples.

It is obvious from Table 2 that the values of ΔH_{pp} decreased from 621 to 117 mT and the values of g-factor increased from 1.52 to 2.65 by increasing Ni content because the g-factor is inversely proportional to the resonance field, according to Equation (1). It is reported that ferrite samples exhibit a low resonance field due to crystalline anisotropy [25]

The value of the Landé g-factor can be calculated by using the following Equation:

$$g \text{ factor} = \frac{h\nu}{\mu_B B_0} \quad (6)$$

where, h is Planck’s constant, ν is a microwave frequency, μ_B is the Bohr magnetron, and B_0 is an applied magnetic field, g-factor value for free electrons is $g = 2.0023$.

The relaxation time is correlated with the line width of ESR. The spin–spin relaxation process is the energy difference(ΔE) transferred to neighbouring electrons and the relaxation time(τ_2) can be determined from the peak to peak line width according to the relation given below. The spin–spin relaxation time(which arises from the influence of one magnetic ion on another)limits the broadening of line width. [26]

$$\frac{1}{T_2} = \frac{\pi g \mu_B \Delta H}{h} \quad (7)$$

Table 2. Peak to peak line width(ΔH_{pp}), g-value, resonance field (H_r), relaxation time(τ_2) of S1,S2,S3 (x=0, 0.2,1.0) samples

Samples	ΔH_{pp} (mT)	H_r (mT)	g-factor	Relaxation time T_2
Co Fe ₂ O ₄	621	445.7	1.52	2.41137x10 ⁻¹¹
Co _{0.8} Ni _{0.2} Fe ₂ O ₄	567.4	432.25	1.56	2.57129 x10 ⁻¹¹
Ni Fe ₂ O ₄	117	254.1	2.65	7.3223x10 ⁻¹¹

3.4 FTIR FOURIER TRANSFORMS INFRARED SPECTROSCOPY (FTIR) STUDIES

IR transmittance spectra of S1,S2,S3 (x=0,0.2,1.0) samples were recorded in 4000–400 cm⁻¹ region at ambient temperature by sol gel method, but only range of 1000– 400cm⁻¹ is shown in Fig.4. In 600 – 400cm⁻¹ wavenumber range, the broad metal–oxygen bands are observed in the FTIR spectra of all samples. The peaks in the range of 600–550 cm⁻¹ region is detected due to tetrahedral metal–oxygen stretching vibration and the peaks in the range of 450–385 cm⁻¹ region arises from the metal– oxygen stretching vibration at the octahedral sites by sol gel method [27]. The presence of the peaks in later i.e. octahedral sits is explained by the cation exchange between the tetrahedral and octahedral spinel sites which often occurs for ferrite [28]. The spectra show no peaks in the range of 4000 cm⁻¹ to 600 cm⁻¹ in the spectra (hence avoided in Fig.4), due to no moisture present in the samples there were no water stretching and bending modes respectively of free or absorbed water. The intensity and position of these modes of vibration (slight shifts in peaks) vary with nickel, cobalt and iron oxide compound concentration due to change in crystalline field effect and strain in the lattice reported in paper[29] The peaks in the 300 to 700 cm⁻¹ regions are assigned to the fundamental vibrations of the ions of the crystal lattice. For analysis of spectra in Fig 4 it is necessary to consider the vibrational spectrum of periodic structures. The vibrational problem is most conveniently treated by classification of crystals according to the continuity of bonding as (1) continuously bonded; (2) discontinuously bonded; and (3) intermediate. In continuously bonded crystals, the atoms are bonded to all nearest neighbors by equivalent forces (ionic, covalent, or van der Waals) and the frequency distribution of vibrations. In the discontinuously bonded or molecular crystal, sets of atoms are tightly bound by (intramolecular) chemical valence forces and separated from adjacent sets by weak (intermolecular) van der waals forces. In the intermediate case the intermolecular forces may be stronger than the actual molecule leading to the overlap, vibrational problem tending to perturbation case [30]

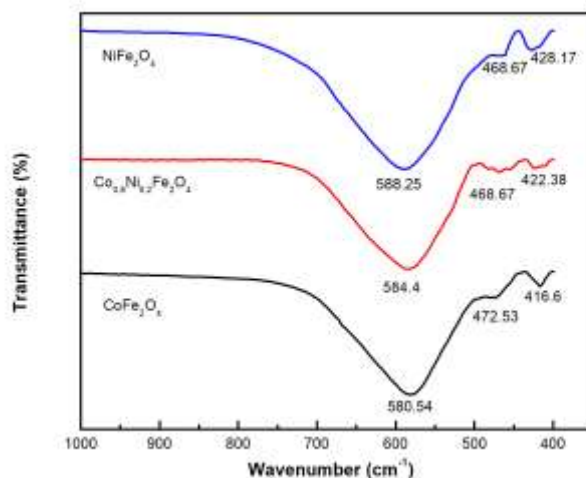


Fig.4 FTIR spectrum of S1,S2,S3(x=0, 0.2,1.0) samples

The transmission peaks observed are as follows:

Table 2 Transmission peaks by FT-IR

Samples	Peak1	Peak2	Peak3
Co Fe ₂ O ₄	580.54 cm ⁻¹	472.53 cm ⁻¹	416.60 cm ⁻¹
Co _{0.8} Ni _{0.2} Fe ₂ O ₄	584.4 cm ⁻¹	468.67cm ⁻¹	422.38 cm ⁻¹
Ni Fe ₂ O ₄	588.25 cm ⁻¹	468.67 cm ⁻¹	428.17 cm ⁻¹

4. CONCLUSIONS

Nickel-substituted cobalt Ferrite nanoparticles are prepared by sol-gel method. These particles belonged to the cubic spinel structure as established by XRD studies. The crystallite size of the nano ferrites found in the range 25 - 34

nm. It is observed that lattice parameters of the samples decreased with increasing Ni content due to the smaller ionic radius of Ni. SEM images show that the particles are agglomerated.

The ESR spectra show a single broad signal indicating the presence of metal ions. It is observed there is a shift in the resonant field and variation in line width with the increase in concentration of Ni. It is seen that the peak-to-peak width is narrow for higher concentration of Ni. The observed g-value from ESR is approximately equal to standard value. The observed peaks in FTIR spectra also confirm the formation of ferrites. FTIR studies reveal cationic exchange in tetrahedral and octahedral interstitial sites.

5. ACKNOWLEDGEMENT

The authors are grateful to University of Mumbai for funding this project under Minor Research Grant, Research center of Guru Nanak College of Arts, Commerce and Sciences, Mumbai, and IIT for FTIR and ESR facilities, Mumbai, for supporting this research work.

6. REFERENCES

- [1]. Kannipamula Vijaya Babu, Matangi Ravi Chandra, Gondu Venkata Santosh Kumar, Kantamsetti Jagadeesh, Effect of cobalt substitution on structural, electrical and magnetic properties of NiFe₂O₄, Processing and Application of Ceramics 11 [1] (2017) 60–66
- [2]. Francisco Augusto Tourinho, Raymonde Franck, Rene Massart, Aqueous ferrofluids based on manganese and cobalt ferrites, Journal of materials Science, 25, 1990, 3249-3254
- [3]. F. Mazaleyrat, L.K. Varga, Ferromagnetic nanocomposites, Journal of Magnetism and Magnetic Materials 215 - 216 (2000) 253-259, DOI: 10.1016/S0304-8853(00)00128-1
- [4]. M. Madhukara Naik, H. S. Bhojya Naik, G. Nagaraju, M. Vinuth, K. Vinu, S. K. Rashmi, Effect of aluminium doping on structural, optical, photocatalytic and antibacterial activity on nickel ferrite nanoparticles by sol-gel auto-combustion method, Journal of Materials Science: Materials in Electronics, 2018,
- [5] Noppakun Sanpo, Christopher C. Berndt, Cuie Wen, James Wang, Transition metal-substituted cobalt ferrite nanoparticles for biomedical applications, Acta Biomaterialia, 9, 2013, 5830–5837,
- [6] Hsing-Cheng Lu, Juu-En Chang, Weng-Wa Vong, Hung-Ta Chen, Ying-Liang Chen, Porous ferrite synthesis and catalytic effect on benzene degradation, International Journal of the Physical Sciences 6(4), 2011, 855-865
- [7] D. Jamon, F. Donatini, A. Siblino, F. Royer, R. Perzynski, V. Cabuil, S. Neveu, Experimental investigation on the magneto-optic effects of ferrofluids via dynamic measurements, Journal of Magnetism and Magnetic Materials, 321, 2009, 1148–1154,
- [8] N. Rezlescu, N. Iftimie, E. Rezlescu, C. Doroftei, P.D. Popa, Semiconducting gas sensor for acetone based on the fine grained nickel ferrite, Sensors and Actuators B 114 (2006) 427–432
- [9] Yaswanth K. Penke, Ganapathi Anantharaman, Janakarajan Ramkumar and Kamal K. Kar, Aluminum substituted nickel ferrite (Ni–Al–Fe): a ternary metal oxide adsorbent for arsenic adsorption in aqueous medium, RSC Adv., 2016, 6, 55608
- [10] Abbas Khaleel, Pramesh N. Kapoor and Kenneth J. Klabunde, Nanocrystalline metal oxides as new adsorbents for air purification, Nanostructured Materials, 11, 1999, 459–468
- [11] Z. Karimi, Y. Mohammadifar, H. Shokrollahi, Sh. Khameneh Asl, Gh. Yousefi, L. Karimi, Magnetic and structural properties of nanosized Dy-doped cobalt ferrite synthesized by co-precipitation, Journal of Magnetism and Magnetic Materials 361, 2014, 150–156,
- [12] L. R. Gonsalves, V. M. S. Verenkar, Synthesis and characterization of nanosize nickel-doped cobalt ferrite obtained by precursor combustion method, Journal of Thermal Analysis and Calorimetry, 108, 2012, 877–880
- [13] W. Wolski, E. Wolska, J. Kaczmarek, P. Piszora, Formation of Manganese Ferrite by Modified Hydrothermal Method, physica status solidi (a) 152, 1995, 19-22.
- [14] Daliya S. Mathew, Ruey-Shin Juang, An overview of the structure and magnetism of spinel ferrite nanoparticles and their synthesis in microemulsions Chemical Engineering Journal, 129, 2007, 51–65
- [15] F. Padella, C. Alvani, A. La Barbera, G. Ennas, R. Liberatore, F. Varsano, Mechano-synthesis and process characterization of nanostructured manganese ferrite, Materials Chemistry and Physics, 90, 2005, 172–177.
- [16] M. Chithra, C.N. Anumol, Baidyanath Sahub, Subasa C. Sahoo, Exchange spring like magnetic behavior in cobalt ferrite nanoparticles Journal of Magnetism and Magnetic Materials, 401, 2016, 1–8
- [17] M. Goodarz Naseri, E. Bin Saion, H. Abbastabar Ahangar, M. Hashim, A.H. Shaari, Synthesis and characterization of manganese ferrite nanoparticles by thermal treatment method, Journal of Magnetism and Magnetic Materials 323 (2011) 1745–1749

- [18] Kamellia Nejati and Rezvanh Zabihi, Preparation and magnetic properties of nano size nickel ferrite particles using hydrothermal method, *Chemistry Central Journal* 6,2012,23
- [19] Ashok Kumar, Pawan S. Rana, M.S.Yadav, R.P.Pant, Effect of Gd³⁺ ion distribution on structural and magnetic properties in nano-sized Mn–Zn ferrite particles, *Ceram. Int.*, 41, 2015, 1297–1302
- [20] Uday Bhasker Sontu, Vijayakumar Yelasani, Venkata Armani Reddy Musugu, Structural, electrical and magnetic characteristics of nickel substituted cobalt ferrite nano particles, synthesized by self combustion method, *J.Magn.Magn.Mater.*,374, 2015,376–380
- [21] G. Mustafa, M.U. Islam, M. Ahmad, W. Zhang, Y. Jamil, A.W. Anwar, M. Hussain, Investigation of structural and magnetic properties of Ce³⁺- substituted nanosized Co–Cr ferrites for a variety of applications. *Journal of Alloys and Compounds J. Alloy. Compd.* 618, 428 -436, 2015
- [22] Suresh Sagadevan, Zaira Zaman Chowdhury, Rahman F. Rafique, Preparation and Characterization of Nickel ferrite Nanoparticles via Co-precipitation Method, *Materials Research...*,2018; 21(2) 1-5,
- [23] Xuebo Cao, and Li Gu Spindly cobalt ferrite nanocrystals: preparation, characterization and magnetic properties, *Nanotechnology* 16 (2005) 180–185, INSTITUTE OF PHYSICS PUBLISHING
- [24] K. Vijaya Babu , G. Satyanarayana , B. Sailaja , G.V. Santosh Kumar , K. Jalaiah , M. Ravi Structural and magnetic properties of Ni_{0.8}M_{0.2}Fe₂O₄ (M = Cu, Co) nano-crystalline ferrites, *Results in Physics* 9 (2018) 55–62
- [25] Chien-Yie Tsay, Yi-Chun Chiu and Chien-Ming Lei Hydrothermally Synthesized Mg-Based Spinel Nanoferrites: Phase Formation and Study on Magnetic Features and Microwave Characteristics, *Materials* 2018, 11, 2274;
- [26] K.K. Bamzai , Gurbinder Kour , Balwinder Kaur , Manju Arora , R.P.Pant , Infrared spectroscopic and electron paramagnetic resonance studies on Dy substituted magnesium ferrite, *Journal of Magnetism and Magnetic Materials* 345(2013)255–260,
- [27] Ashok Kumar, Nisha Yadav, Dinesh S. Rana, Parmod Kumar, Manju Arora, R.P.Pant, Structural and magnetic studies of the nickel doped CoFe₂O₄ ferrite nanoparticles synthesized by the chemical co-precipitation method, *J.Magn.Magn.Mater.*,394,2015,379–384
- [28] Petrisor Samoila, Corneliu Cojocaru, Igor Cretescu, Catalina Daniela Stan, Valentin Nica, Liviu Sacarescu and Valeria Harabagiu, Nanosized Spinel Ferrites Synthesized by Sol-Gel Autocombustion for Optimized Removal of Azo Dye from Aqueous Solution, *Journal of Nanomater*,2015, 2015, 1-13
- [29] Sandhya S. Bharambe, Ajinkya Trimukhe, Pushpinder Bhatia, Synthesis Techniques of Nickel Substituted Cobalt Ferrites – An Investigative Study Using Structural Data, *Materials Today: Proceedings* 23,2020,373–381
- [30] Petrisor Samoila, Corneliu Cojocaru, Igor Cretescu, Catalina Daniela Stan, Valentin Nica, Liviu Sacarescu and Valeria Harabagiu, Nanosized Spinel Ferrites Synthesized by Sol-Gel Autocombustion for Optimized Removal of Azo Dye from Aqueous Solution, *Journal of Nanomater*, 2015, 1-13